

A Study On 3D Printer Filament Materials Using LAMMPS Simulator

Junseo Lee¹ and Eunsung Jekal^{*,2}

¹Okdong middleschool, Ulsan, South Korea and

²Physics Department, Jekal's Laboratory, Ulsan, South Korea*

ABSTRACT

Recently, in the era of the 4th Industrial Revolution, the educational field of 3D printers is increasing, and the demand for 3D printers for home use is also increasing. Fused Deposition Modeling (FDM) and Digital Light Processing (DLP) are representative 3D printer's output methods, but the FDM method, which uses filaments as the main material, is inexpensive and convenient to use, so it is widely used for home and education. However, this method tends to waste the amount of filament used due to the support during output, and the problem of long output time has not been solved yet, so there is a need to improve this. This study proposes a "non-support output system" technology by designing several models that can be output without a support through simulation. As a result of the study, the amount of filament, which is the main material, decreased during output, and the output time was rapidly reduced, so it was possible to visually confirm cost reduction and energy saving. Therefore, this study seems to be of great significance in that it suggested a direction for the development of 3D printers that supplement and improve the shortcomings of existing 3D printers.

Date of Submission: 20-07-2023

Date of Acceptance: 30-07-2023

I. INTRODUCTION

A. Definition of 3D Printer

It refers to a machine that creates three-dimensional objects based on input drawings as if a 2D printer prints a type or picture. [1–3]

B. 3D Printer Output Method

3D printers are divided into stacked and cut types according to the method of making three-dimensional printed materials. The stacked type is a method of stacking a very thin two-dimensional surface in layers, and the cutting type is to make a print by cutting a large lump as if it were carved. In the case of a cutting type, unnecessary parts of the material are cut off, so the material is lost, and the surface of the part to which the support is connected is not smooth because of the support that prevents shape change when pulling out the object. However, most of the recent 3D printers are stacked printers. [4, 5]

C. Definition of support

It refers to floor supports and shape aids that are needed to print products on a 3D printer.

II. MOTIVATION FOR RESEARCH

When outputting a result with a 3D printer, a support is required to support the overhang (floating part in the air) so that it does not flow down. Therefore, the results and support are produced together with a 3D printer, which increases the amount of filaments (materials of the 3D printer) and output time used to make the support. Many people always feel uncomfortable about that when they make things with 3D printers. Support had to always be used to support overhang, and because of the nature of the 3D printer, even small printouts take a lot of time, but with the addition of time to produce support, you have to spend more time waiting for a long time. In addition, the time it takes to remove the support of the output and the time for post-processing after removing it may be wasted. Therefore, to solve this problem, the purpose of this study is to devise a method that can output an object to a 3D printer by utilizing a material that hardens relatively quickly. [6, 7]

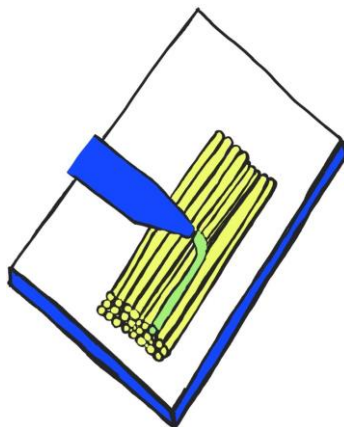


FIG. 1. An illustration that expresses the operating principles of stacked 3D printers.

III. PREVIOUS RESEARCH AND INVESTIGATION

A. Problems and Improvement Methods

Currently, in stacked 3D printers, the object output using the support is not melted but hardened to form a shape, and then the support is removed to output the object we want. There are two main types of filaments for 3D printers, the first being Acrylonitrile Butadiene Styrene copolymer (ABS). As its name suggests, it is a styrene resin composed of three components: acrylonitrile, butadiene, and styrene. The second is Poly Lactic Acid (PLA). It is a plastic made of corn starch, and bio-polyester is the main ingredient. However, both types do not harden quickly, requiring support during output. This study used Bulk Metallic Glass (BMG) to improve this problem. BMG is a recently made new material that is very flexible and has glass properties, not plastic, so it is considered suitable for this study because it hardens much faster than existing plastic filaments[8–11].

IV. METHODOLOGY

The MD simulation presently carried out use the

OVITO

OVITO makes molecular dynamics simulations visual. Molecular dynamics (MD) is a standard simulation technique for predicting materials structures and behavior at the atomic scale. This type of simulation model computes three-dimensional particle trajectories, which typically need to be further analyzed in order to obtain scientific insights from the data. Powerful analysis and visualization techniques play a key role in this process as the simulated systems become bigger and more complex. Without the right software tool, key information would remain undiscovered, inaccessible and unused. OVITO is a visualization and analysis software for output data generated in molecular dynamics, atomistic Monte-Carlo and other particle-based simulations.

B. Sample preparation

In MD simulations, we select the values presented in Tripathy et. al for potential energy expressions between molecules. Based on the van der Waals energy value between the magnetic particles, the calculation was conducted by converting to the following Lenard-Jones potential.

Large-scale Atomic/Molecular Massively Parallel Simulator (LAMMPS) package[12]. Atomistic visualization and analysis is done with the Open Visualization Tool (OVITO) visualization software[13].

A. LAMMPS

LAMMPS is a classical molecular dynamics (MD) code that models ensembles of particles in a liquid, solid, or gaseous state. It can model atomic, polymeric, biological, solid-state (metals, ceramics, oxides), granular, coarse-grained, or macroscopic systems using a variety of interatomic potentials (force fields) and boundary conditions. It can model 2d or 3d systems with sizes ranging from only a few particles up to billions. In the most general sense, LAMMPS integrates Newton's equations of motion for a collection of interacting particles. A single particle can be an atom or molecule or electron, a coarse-grained cluster of atoms, or a mesoscopic or macroscopic clump of material. The interaction models that LAMMPS includes are mostly short-ranged in nature. LAMMPS uses neighbor lists to keep track of nearby particles. The lists are optimized for systems with particles that are repulsive at short distances, so that the local density of particles never becomes too large. This is in contrast to methods used for modeling plasma or gravitational bodies (like galaxy formation)[9, 14, 15].

Among the parameters used in Eqn. (1), the value of PEEK between particles is described in Table 1. Here, ϵ_{LJ} and σ_{LJ} represent the depth of the well of the Leonard-Jones potential and the distance between the

particles to which the potential energy becomes 0, and m_{bead} represents the mass of a single particle. For parameters applied between the PEEK particles and the surface, $3\epsilon_{LJ}$ was used to be attached between the bottom plate, and $1\epsilon_{LJ}$ was used for the upper plate. In the case of σ_{LJ} , both plates used $1\sigma_{LJ}$.

As shown in Figure 2, the simulation system consists of 339 linear chain molecules with 100 beads. It consists of a Face Centered Cubic (FCC) type upper plate and a floor plate modeled with a rigid body. At this time, the size of the beads constituting the molecule and the flat plate was $1\sigma_{LJ}$. The boundary condition used the periodic boundary condition in all directions, and the size of the system to which the periodic condition was applied was $14.142 \times 14.142 \times 140$. Basically, the system temperature was maintained using the Langevine thermostat to meet the conditions of the canonical ensemble. The time step of the simulation was 0.01τ , and the system temperature was initially set to $T=5$ for molecular dispersion, and then it was cooled back to the desired temperature, $T=1$, after 5×10^5 step. Finally, post-treatment was performed using the data obtained, and the shape was analyzed.

V. RESULTS AND DISCUSSIONS

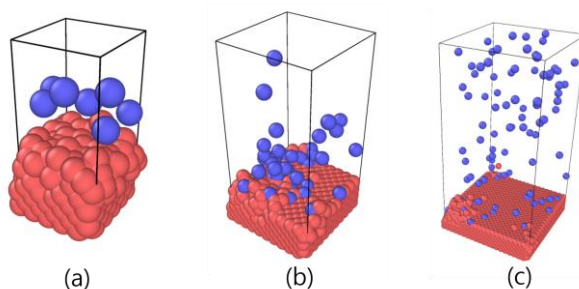


FIG. 2. Snapshot of a periodic cells with different size

The present work employs a number of well-known local atomic structural measures: Figure 3 graphically shows the value of the Radial Pair Distribution Function ($g(r)$) between the floor plane and the molecular PEEK and PEEK molecules according to the temperature of the system according to the applied simulation model. $g(r)$ represents a density that changes according to a particle distance to be measured for a reference particle. The comparative temperature condition was compared with a temperature up to 10 times higher than the reference temperature, $T=1$. As shown in Fig. 3, both high and low temperature results are present at the first local maximum $r=0.7$, that is, the interval value between beads forming a chain molecule, and the next appears before and after $r=2.2\sigma_{LJ}$. On the other hand, in Fig. 4, which shows the results of simulations that have grown in size, it exists even before and after $r=1.1\sigma_{LJ}$, indicating that there is entanglement due to manpower. In this model, the local maximum is similar even under other temperature conditions, and in a low temperature environment, the local maximum is increased near $r=1.1$, resulting in increased structuralization. This is thought to be due to irregular and dissipative forces in the attraction between molecules. In particular, in the case of dissipative forces, information on speed as well as distance is included, indicating that it is a suitable model for predicting dynamic changes or homogeneous structures rather than interpreting static structures. On the other hand, small models basically have van der Waals attraction, so if the degree of disturbance due to system temperature is less than the intermolecular potential energy value, a structure such as an internal void may occur.

Figure 5 shows the cavity-shaped pores generated according to the system temperature during the MD simulation. In order to show the part where the pores appear, an area was organized so that the thickness was $y=2\sigma_{LJ}$ in the direction, and the part where the pores occurred was shown. As illustrated in the figure, in the case of high temperatures $T=10$ and $T=5$, molecules were expanding steadily, but pores were not manifested, and as the temperature dropped to $T=2$ and $T=1$, pores with a diameter of $5-10\sigma_{LJ}$ were generated. For the diameter of the pores, the range was estimated by calculating the average value of the maximum minimum diameter of each empty space present in the figure. It is inferred that the PEEK molecules, which are the units that make up the structure, have a long chain shape in the longitudinal direction, and that voids form when entanglement by attraction existing between the molecules occurs partially unevenly.

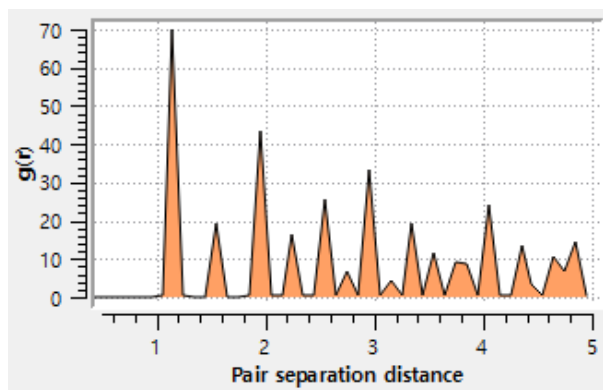


FIG. 3. Radial Distribution Functions for large model simulation.

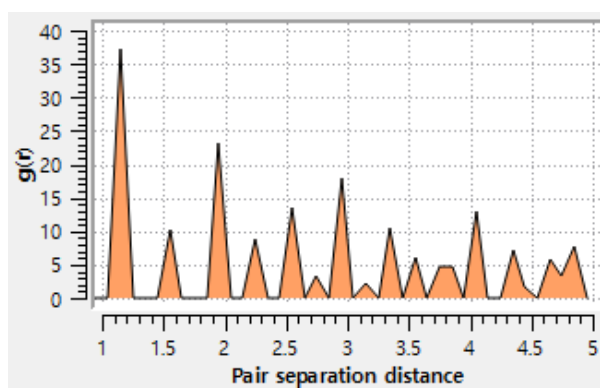


FIG. 4. Radial Distribution Functions for small model simulation

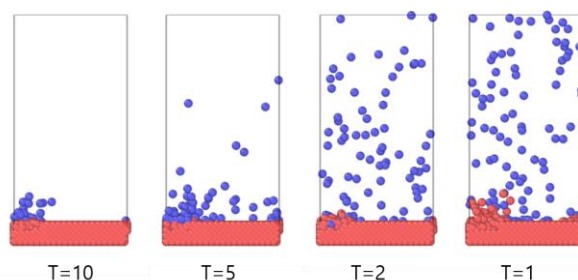


FIG. 5. Snapshots of temperature-dependent cavity distributions

1) Changes in data values according to differences in atomic size According to the graph, TotEng had a value of -7 to -5, E-pair also had a value of -7 to -5, and temp had a value of 0 to 1, but Press had a small change and difference in the graph, which was about 0.2 on average and larger in the middle. 2) Changes in data values according to the amount of atoms accumulated Analyzing the data values in the case of 1,500 and 5,700 accumulated atoms, respectively, TotEng had an average value of -7 to -6, and the same was true in the case of E-pair's graph, but the slope of 5,700 was slightly sharper. In the case of Press's graph, the average value of the graph was about 0.2 different from the average value of 1 in the case of 1500 graphs, but in the case of 5,700 graphs, the slope was gradually gentle at 8.5 and inversely proportional to stop at 3.

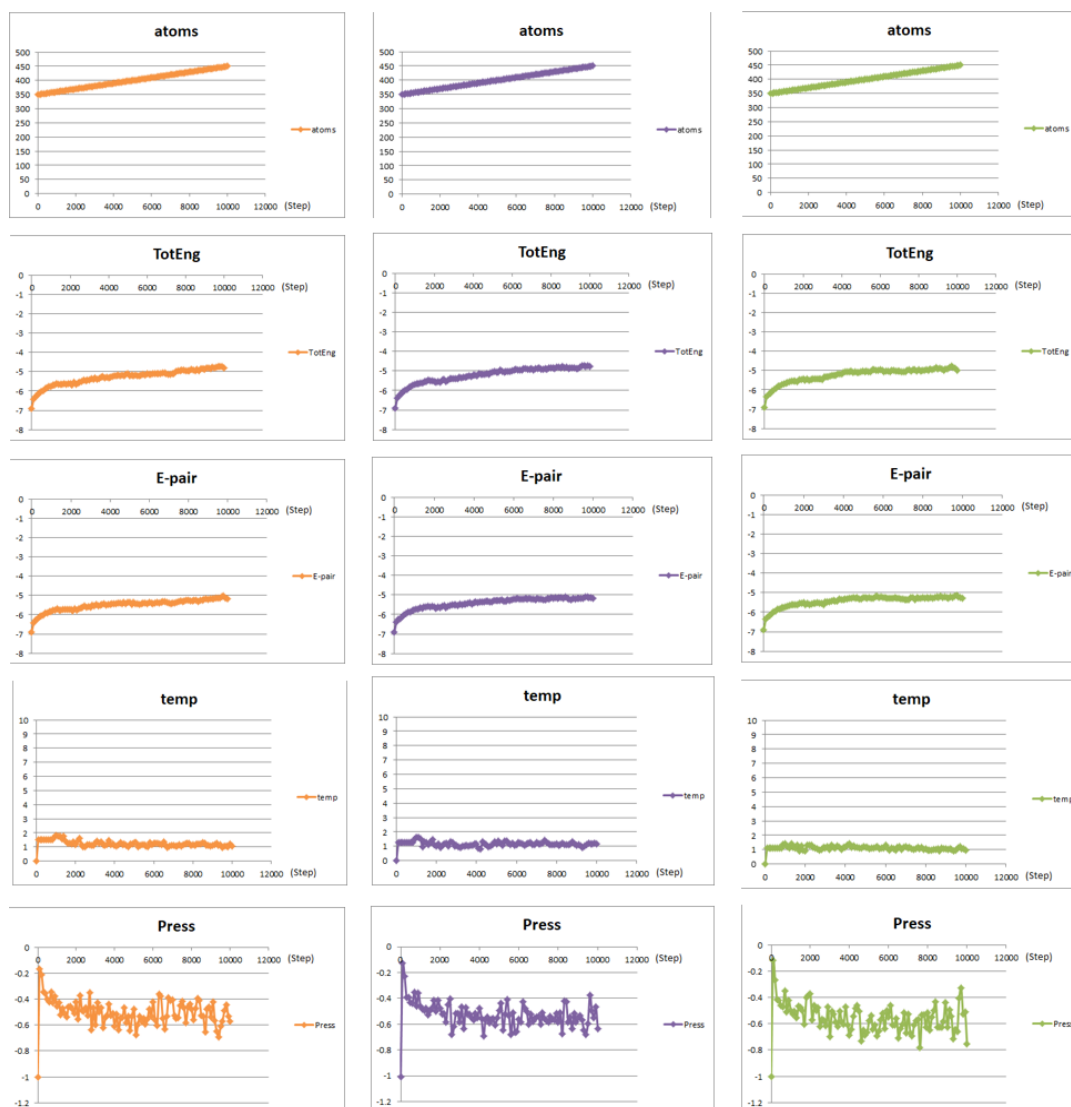


FIG. 6. Snapshots of temperature-dependent cavity distributions

VI. CONCLUSION

The following conclusions were obtained by deriving simulation results on entanglement and co-occurrence according to temperature of PEEK chain molecules implemented using molecular dynamics.

The $g(r)$ results show that intermolecular entanglement can only be confirmed in interpretation with the model as the base MD half. On the other hand, when the DPD model was applied, the molecules were spatially homogenized.

Through MD simulation, it was observed that the volume was reduced and voids were generated inside through the process of solidifying molecules in a high-temperature PEEK melting state.

It was confirmed that MD simulation is a reasonable method for observing non-uniform structures generated during the coagulation process and pores generated by them.

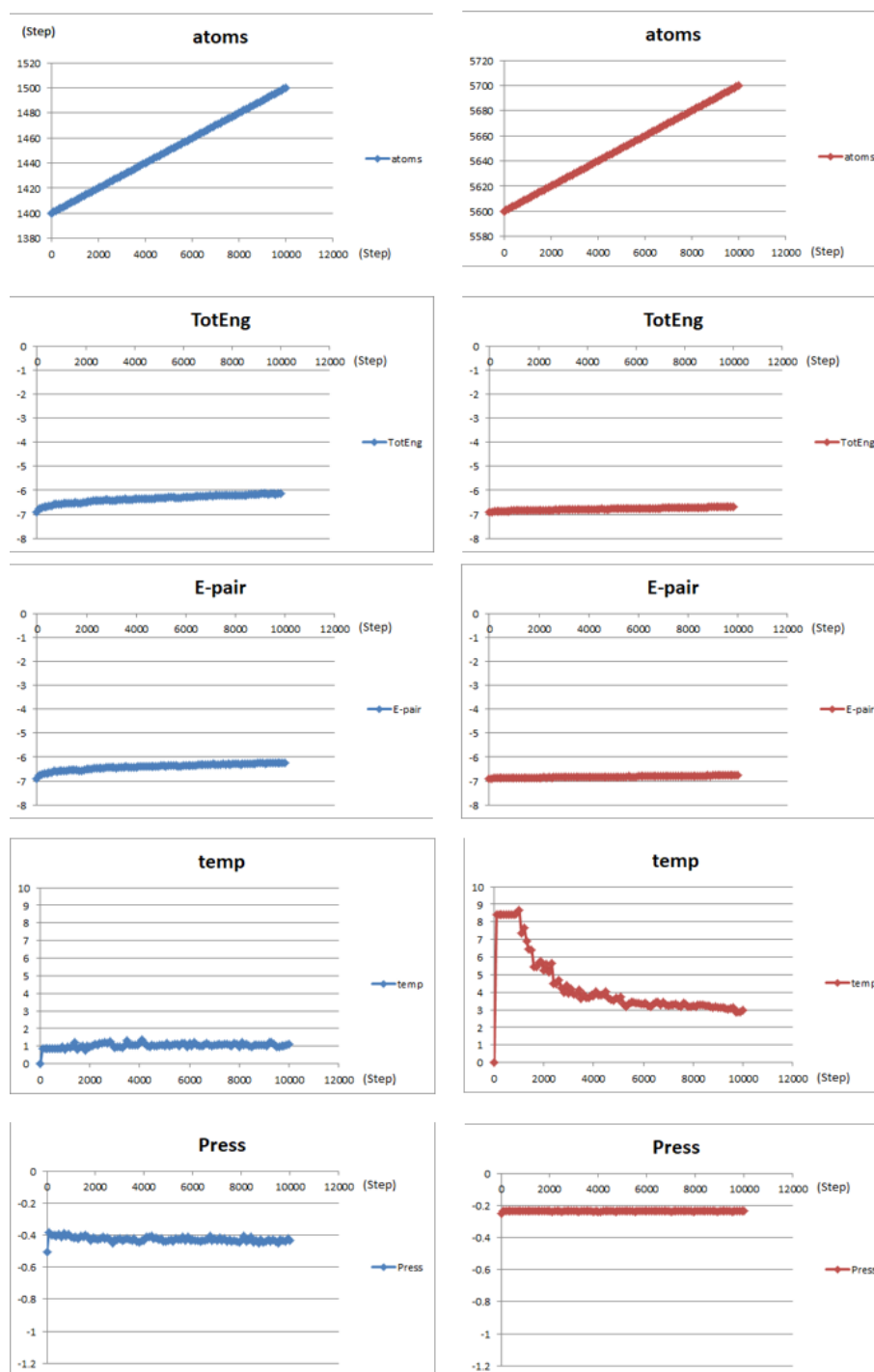


FIG. 7. Snapshots of temperature-dependent cavity distributions

REFERENCES

- [1]. B. P'Erez, H. Nykvist, A. F. Brøgger, M. B. Larsen, And M. F. Falkeborg, Impact Of Macronutrients Printability And 3d-Printer Parameters On 3d-Food Printing: A Review, *Food Chemistry* 287, 249 (2019).
- [2]. C. Schubert, M. C. Van Langeveld, And L. A. Donoso, Innovations In 3d Printing: A 3d Overview From Optics To Organs, *British Journal Of Ophthalmology* 98, 159 (2014).
- [3]. N. Shahrubudin, T. C. Lee, And R. Ramlan, An Overview On 3d Printing Technology: Technological, Materials, And Applications, *Procedia Manufacturing* 35, 1286 (2019).
- [4]. D. Roberson, D. Espalin, And R. Wicker, 3d Printer Selection: A Decision-Making Evaluation And Ranking Model, *Virtual And Physical Prototyping* 8, 201 (2013).
- [5]. M. E. Mackay, Z. R. Swain, C. R. Banbury, D. D. Phan, And D. A. Edwards, The Performance Of The Hot End In A Plasticating 3d Printer, *Journal Of Rheology* 61, 229 (2017).
- [6]. T. Letcher And M. Waytashek, Material Property Testing Of 3d-Printed Specimen In Pla On An Entry-Level 3d Printer, In *Asme International Mechanical Engineering Congress And Exposition*, Vol. 46438 (American Society Of Mechanical Engineers, 2014) P.

- V02at02a014.
- [7]. W. Oropallo And L. A. Piegl, Ten Challenges In 3d Print- Ing, *Engineering With Computers* 32, 135 (2016).
 - [8]. A. Manoj, R. Ch, Et AL., Biodegradable Filament For 3d Printing Process: A Review, *Engineered Science* 18, 11 (2022).
 - [9]. J. Hergel And S. Lefebvre, Clean Color: Improving Multi- Filament 3d Prints, In *Computer Graphics Forum*, Vol. 33 (Wiley Online Library, 2014) Pp. 469–478.
 - [10]. J. Zhan, T. Tamura, X. Li, Z. Ma, M. Sone, M. Yoshino,
 - [11]. S. Umezu, And H. Sato, Metal-Plastic Hybrid 3d Print- Ing Using Catalyst-Loaded Filament And Electroless Plating, *Additive Manufacturing* 36, 101556 (2020).
 - [12]. S. Hassanifard And S. M. Hashemi, On The Strain-Life Fa- Tigue Parameters Of Additive Manufactured Plastic Mate- Rials Through Fused Filament Fabrication Process, *Additive Manufacturing* 32, 100973 (2020).
 - [13]. A. P. Thompson, H. M. Aktulga, R. Berger, D. S. Bolintineanu, W. M. Brown, P. S. Crozier, P. J. In't Veld, A. Kohlmeyer, S. G. Moore, T. D. Nguyen, Et AL., Lammops-A Flexible Simulation Tool For Particle-Based Ma- Terials Modeling At The Atomic, Meso, And Continuum Scales, *Computer Physics Communications* 271, 108171 (2022).
 - [14]. A. Stukowski, Visualization And Analysis Of Atomistic Simulation Data With Ovito–The Open Visualization Tool, *Modelling And Simulation In Materials Science And Engi- Neering* 18, 015012 (2009).
 - [15]. R. Freitas, M. Asta, And M. De Koning, Nonequilibrium Free-Energy Calculation Of Solids Using Lammops, *Compu- Tational Materials Science* 112, 333 (2016).
 - [16]. B. Frantzdale, S. J. Plimpton, And M. S. Shephard, Soft- Ware Components For Parallel Multiscale Simulation: An Example With Lammops, *Engineering With Computers* 26, 205 (2010).
 - [17]. M. T. Humbert, Y. Zhang, And E. J. Maginn, Pylat: Python Lammops Analysis Tools, *Journal Of Chemical In- Formation And Modeling* 59, 1301 (2019).